

Spin transport in the XXZ model at high temperatures: Classical dynamics versus quantum $S = 1/2$ autocorrelations

ROBIN STEINIGEWEG^(a)

J. Stefan Institute - Jamova 39, SI-1000 Ljubljana, Slovenia, EU

PACS 75.10.Pq – Spin chain models
 PACS 05.60.Cd – Classical transport
 PACS 05.60.Gg – Quantum transport

Abstract. - The transport of magnetization is analyzed for the classical Heisenberg chain at and especially above the isotropic point. To this end, the Hamiltonian equations of motion are solved numerically for initial states realizing harmonic-like magnetization profiles of small amplitude and with random phases. Above the isotropic point, the resulting dynamics is observed to be diffusive in a hydrodynamic regime starting at comparatively small times and wave lengths. In particular, hydrodynamic regime and diffusion constant are both found to be in quantitative agreement with close-to-equilibrium results from quantum $S = 1/2$ autocorrelations at high temperatures. At the isotropic point, the resulting dynamics turns out to be non-diffusive at the considered times and wave lengths.

Transport in one-dimensional systems has been a topic of theoretical investigations for several decades, and even nowadays there is an ongoing and still increasing interest in understanding transport phenomena in such systems, including their dependence on temperature [1–27]. Much work has been devoted to a qualitative classification of the dynamics into either non-normal ballistic or normal diffusive behavior. In this context the crucial mechanisms for the emergence of pure diffusion have been addressed and non-integrability is frequently discussed w.r.t. its role as a basic prerequisite, see [4], for instance. Particularly, spin chain models are a central issue of research [4–27], with a considerable focus on transport of magnetization (spin) in the anisotropic $S = 1/2$ Heisenberg chain [4–22], which serves as a prototype model due to its integrability in terms of the Bethe ansatz [28]. The specific question of spin transport in this model has experienced an upsurge of interest during the last decade, not least motivated by experiments on low-dimensional quantum magnets, where large magnetic heat conduction [29–31] and long nuclear magnetic relaxation times [32,33] have been observed. But still, despite much effort, spin transport in the anisotropic $S = 1/2$ Heisenberg chain is not fully understood yet, not even for finite anisotropies $\Delta \neq 0$.

So far, many works have focused on the dynamics of

magnetization in the limit of both zero momentum and frequency in connection with the spin Drude weight, see, e.g., [5–9]. While non-zero Drude weights for $\Delta < 1$ [8] imply partially ballistic dynamics [4] (for $\Delta = 0$ completely ballistic dynamics) and prevent the occurrence of purely diffusive dynamics at zero momentum and frequency, they do not allow for conclusions on diffusion laws at finite momentum. Early analysis of the time-dependent correlation function of the local spin density [10] suggested the absence of diffusion for all anisotropies $0 \leq \Delta \leq 1$ in the high-temperature limit $T = \infty$, see also [11]; however, recent low-temperature studies at the isotropic point $\Delta = 1$, using bosonization and transfer matrix renormalization group [4] as well as Monte Carlo [12], are consistent with finite-frequency diffusion at small momentum. On the other hand, $T = \infty$ investigations at $\Delta = 1$ [13] on the basis of the Lindblad quantum master equation point to superdiffusive dynamics. But diffusion is found in this approach for anisotropies $\Delta > 1$ [13–15] with a high-temperature diffusion coefficient which is in quantitative agreement with time-dependent perturbation theory for the current autocorrelation in the limit of zero momentum [16,17]. Further analysis of the spin density autocorrelation at $\Delta > 1$ [18] demonstrated finite-time diffusion at small momentum also for lower temperatures $T < \infty$; however, the spectrum of the zero-momentum current autocorrelation might still feature low-frequency anomalies

^(a)E-mail: robin.steinigeweg@ijs.si

indicative for an insulator [19, 20].

In this work we will shed light on the high-temperature dynamics of magnetization in a different way, namely, by applying classical mechanics. Certainly, the application of classical mechanics is not a novel concept; however, most work has focused on correlation functions at the isotropic point $\Delta = 1$ yet [23–27] without providing a quantitative comparison to quantum mechanics and $S = 1/2$, which cannot be considered as a classical limit a priori, even at high temperatures $T = \infty$. Here, we will provide such a comparison, motivated by a possibly simple scaling of correlation functions with S [16], and we will particularly unveil a convincing quantitative agreement at $\Delta > 1$. Due to this agreement, our results suggest that signatures of quantum $S = 1/2$ diffusion at $\Delta > 1$ [13–18] can be indeed understood as a “classical” phenomenon.

The present paper is structured as follows: First of all, we will give the pertinent definitions by introducing the anisotropic Heisenberg chain in general and in particular the corresponding Hamiltonian equations of motion in the case of classical mechanics. Thereafter we will establish a transport scenario by specifying a certain class of initial states with inhomogeneous magnetization profiles of small amplitude. We will afterwards continue by discussing the properties of diffusive dynamics and in this context we will briefly review close-to-equilibrium results on diffusion at high temperatures in the case of quantum mechanics and $S = 1/2$. To these results we will eventually compare our numerical findings on classical mechanics, starting above but also proceeding to the isotropic point. We will finally close with a summary.

In this work we investigate the anisotropic Heisenberg chain (XXZ model) with a Hamiltonian of the form

$$H = J \sum_r^L (S_r^x S_{r+1}^x + S_r^y S_{r+1}^y + \Delta S_r^z S_{r+1}^z), \quad (1)$$

where S_r^i ($i = x, y, z$) are the components of the spin \mathbf{S}_r at site r , L denotes the number of sites, J represents the exchange coupling constant, and Δ is the anisotropy parameter.

In the case of classical mechanics (CM) the spins \mathbf{S}_r are three-dimensional vectors of unit length, $|\mathbf{S}_r| = 1$, and their dynamics is generated by the Hamiltonian equations of motion [23–27]

$$\dot{\mathbf{S}}_r = \frac{\partial H}{\partial \mathbf{S}_r} \times \mathbf{S}_r \equiv \mathbf{J}_{r-1} - \mathbf{J}_{r+1} \quad (2)$$

with $\mathbf{J}_{r\pm 1} = \pm J \mathbf{S}_r \times (S_{r\pm 1}^x, S_{r\pm 1}^y, \Delta S_{r\pm 1}^z)$ as the incoming and outgoing spin currents. Since this set of equations is non-integrable in terms of the Liouville-Arnold theorem [34, 35], exact analytical solutions can only be given for mostly trivial initial configurations. We thus solve the set of equations numerically using a 4th order Runge-Kutta algorithm with a fixed time step of $\delta t J = 0.01$; however, the presented results in the work at hand will not depend

on this particular choice of the time step, cf. [23–27].

In order to realize a transport scenario we choose a certain class of initial states with non-homogenous magnetization profiles. Concretely, these initial states read

$$\mathbf{S}_r(0) = \begin{pmatrix} \cos(\alpha_r) \sqrt{1 - A^2 \cos^2(qr)} a_r^z \\ \sin(\alpha_r) \sqrt{1 - A^2 \cos^2(qr)} a_r^x \\ A \cos(qr) a_r^y \end{pmatrix}, \quad (3)$$

where the first term of the z -component is a cosine-shaped magnetization profile at a single momentum $q = 2\pi k/L$ and with the total amplitude $A \in [0, 1]$. The second term of the z -component introduces local amplitudes $a_r \in [0, 1]$ drawn at random from a uniform distribution. This term hence adds contributions at other momenta $q' \neq q$, but the main contribution is still at q . The remaining x - and y -components essentially contain local phases $\alpha_r \in [0, 2\pi]$ drawn at random from a uniform distribution again. We emphasize that Eq. (3) defines a subclass of all possible initial states, which is particularly evident for small total amplitudes $A \ll 1$. Later we will choose a small $A = 1/4$ in order to model “close-to-equilibrium” states. Due to the random choice of local phases α_r , these states correspond reasonably to high temperatures. In fact, also correlation functions at high temperatures are obtained by sampling over a set of completely random configurations, see [26], for instance.

Our aim is to analyze the decay of the q -mode in time, i.e., the relaxation of $S_q^z = \sum_r^L \cos(qr) s_r^z$. For long chains of length $L = 18000$, as considered throughout this work, the initial value $S_q^z(0) \approx N A/4$ does not depend on the concrete realization of the random numbers in Eq. (3) any further; however, the relaxation of S_q^z still differs from one realization to another. We therefore analyze the ensemble average $M_q = 1/N \sum_n^N S_q^z$ over $N = 1000$ different initial states in order to obtain the “typical” dynamics. One may expect that each S_q^z is close to the ensemble average M_q in the thermodynamic limit $L \rightarrow \infty$. In fact, this expectation is supported because our results for M_q at large q can be reproduced for $L \ll 18000$ if $N \gg 1000$. In other words, the shorter the chain the more initial states are needed to reach the ensemble average.

The dynamics may be called diffusive if M_q satisfies a (lattice) diffusion equation of the form

$$\dot{M}_q(t) = -\tilde{q}^2 D M_q(t), \quad \tilde{q}^2 = 2[1 - \cos(q)] \sim q^2 \quad (4)$$

with a diffusion constant D , which is independent of both time t and momentum q . Of course, a diffusion equation is expected to be valid solely in a hydrodynamic regime starting at sufficiently long t and small q , e.g., in the limit of $t \rightarrow \infty$ and $q \rightarrow 0$. Hence, in order to investigate the full time- and momentum-dependence of the dynamics, we reformulate Eq. (4) and introduce a generalized diffusion coefficient, which given by [18]

$$D_q(t) = \frac{\dot{M}_q(t)}{-\tilde{q}^2 M_q(t)}. \quad (5)$$

This quantity is in the focus of the present work. It is well defined whenever M_q takes on a non-zero value, otherwise it diverges. Such a divergence naturally emerges after the relaxation of M_q due to “fluctuations” around zero, e.g., as arising from numerical errors; however, we study the dynamics until the relaxation of M_q here. In any case, a divergence of $D_q(t)$ is a clear indication of non-diffusive behavior. It is worth to mention that Eq. (5) is equivalent to writing M_q in the form

$$\frac{M_q(t)}{M_q(0)} = \exp \left[-\tilde{q}^2 \int_0^t dt' D_q(t') \right], \quad (6)$$

which leads to a strictly exponential decay for a diffusion constant $D_q(t) = \text{const.}$

Before presenting results for the case of CM, let us also discuss the case of quantum mechanics (QM) in detail, to which we are going to compare afterwards. In that case, all spins become operators, their time arguments have to be understood with respect to the Heisenberg picture, and initial configurations are specified by a density matrix ρ , which is possibly a pure state. In fact, pure states have been considered in numerical simulations [21] using the time-dependent density matrix renormalization group, yet restricted to zero temperature. In principle the “typical” dynamics can be defined again by the ensemble average $M_q(t) = 1/N \sum_n \text{Tr}[S_q^z(t) \rho]$. Here, however, we decide to proceed in a different way and instead define M_q as the density autocorrelation $M_q(t) = \langle S_q^z(t) S_{-q}^z(0) \rangle$, where the angles denote the canonical equilibrium average at the inverse temperature $\beta = 1/T$, set to $\beta = 0$. This way we are going to compare to linear response theory [36] at high temperatures, i.e., the quantity $D_q(t)$ in Eq. (5) becomes a generalized high-temperature diffusion coefficient close to equilibrium.

We especially make use of the perturbation theory (PT) in [16, 17] for $S = 1/2$ and $\Delta > 1$, which yields a prediction for $D_q(t)$ in the limit of $q \rightarrow 0$. Therein, $D_{q \rightarrow 0}(t)$ is found to take on the constant value $D_{q \rightarrow 0} J = 0.88/\Delta$ at a time scale $t J > 3.0/\Delta$. Moreover, this value has been brought into quantitative agreement with diffusion constants from complementary non-equilibrium bath scenarios [13–15] on the basis of the Lindblad quantum master equation. In addition, $D_q(t) \approx D_{q \rightarrow 0}(t)$ has been observed in [18] at finite momenta $q \lesssim 2\pi/9$, at least at the treatable times $t J \lesssim 10$, using full exact diagonalization (ED) for a chain of length $L = 18$. In view of these findings, the starting point of the following CM simulation will be $\Delta > 1$ and $q = 2\pi/9$.

Now we turn to our CM findings. In Fig. 1 we display the numerical result for the decay of M_q for anisotropies $\Delta = 1.5, 2.0$ at momenta $q = 2\pi/9, \pi/9$, as obtained for a small total amplitude $A = 1/4$. To repeat, we consider a chain of length $L = 18000$ and average over $N = 1000$ initial configurations. Apparently, the decay of M_q takes place at rather short time scales $t J \lesssim 30$. This decay is the faster the larger Δ and the larger q . For comparison,

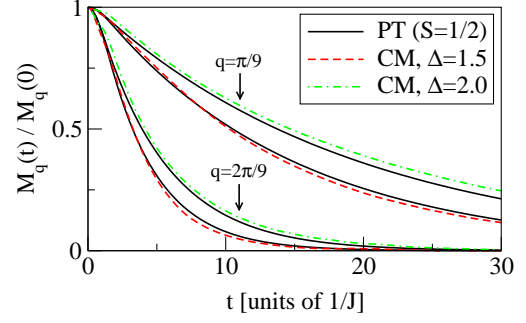


Fig. 1: Relaxation of modes $M_q(t)$ at momenta $q = \pi/9, 2\pi/9$ for anisotropies $\Delta = 1.5, 2.0$ in a chain of length $L = 18000$, as obtained numerically from classical mechanics for the total amplitude $A = 1/4$ (non-solid curves). Numerical parameters: $N = 1000$, $\delta t J = 0.01$. For comparison, the decay of quantum $S = 1/2$ autocorrelations at $\beta = 0$ is shown, as predicted by the $q \rightarrow 0$ perturbation theory in [17] (solid curves).

we additionally indicate the relaxation of $S = 1/2$, $\beta = 0$ density autocorrelations, using Eq. (6), $D_q(t) \approx D_{q \rightarrow 0}(t)$, as well as $D_{q \rightarrow 0}(t)$ according to the PT in [17] (depicted in Fig. 2). The obvious agreement in Fig. 1 is remarkable for several reasons: First, we compare the average decay of a density to the decay of a density autocorrelation. Second, this comparison is done between CM and QM, but generally the quantum problem can only be considered reliably as classical for a sufficiently large spin quantum number S , even in the limit of high temperatures. In any case, the agreement usually requires a proper scaling factor taking into account the different length of a spin in CM and QM. The latter point deserves closer attention since we have not introduced such a scaling factor, i.e., the spins in Eq. (2) are still three-dimensional vectors of unit length. We emphasize that this observation is not an artefact of the applied numerical integrator because later we will reproduce existing CM simulations at $\Delta = 1$.

Next we intend to classify the type of the dynamics in Fig. 1. To this end, the time-dependence of the generalized diffusion coefficient $D_q(t)$ is displayed in Fig. 2 at fixed momentum $q = \pi/9$ for anisotropies $\Delta = 1.5, 2.0$. For a small total amplitude $A = 1/4$ we again find a convincing agreement with $D_{q \rightarrow 0}(t)$ according to the PT in [17]. The CM curve $D_{\pi/9}(t)$ not only takes on an approximately constant value close to $D_{q \rightarrow 0} J = 0.88/\Delta$, but also reaches this value at roughly the same point in time, namely, at $t J \approx 3.0/\Delta$. Clearly, the agreement is better for $\Delta = 1.5$ in Fig. 2(a) than for $\Delta = 2.0$ in Fig. 2(b), where the CM curve $D_{\pi/9}(t)$ slightly decreases for $t J \gtrsim 10$. In order to give insight into the origin of this decrease, we also show $D_{\pi/9}(t)$ for larger total amplitudes $A > 1/4$. Apparently, the decrease is the more pronounced the larger A . Thus, since the parameter A adjusts the total amplitude of the initial magnetization profile, we identify the decrease as a “not-close-to-equilibrium” effect. Even though not shown here, the decrease becomes also more pronounced as Δ

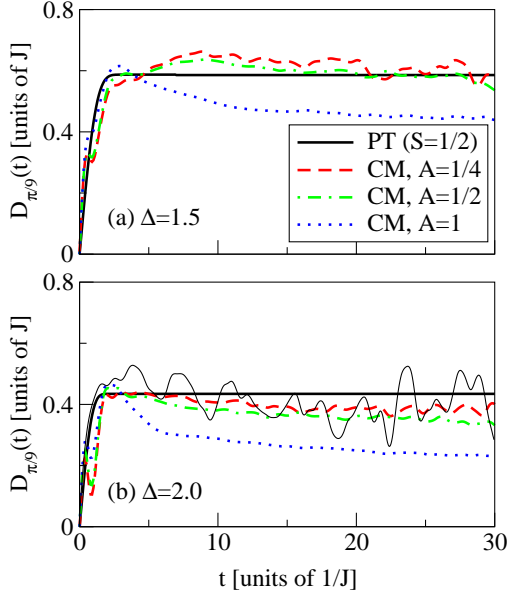


Fig. 2: Time-dependence of the generalized diffusion coefficient $D_{\pi/9}(t)$ for anisotropies (a) $\Delta = 1.5$, (b) 2.0 in a chain of length $L = 18000$, as obtained numerically from classical mechanics for different total amplitudes $A = 1/4$, $1/2$, and 1 (non-solid curves). Numerical parameters: $N = 1000$, $\delta t J = 0.01$. The $q \rightarrow 0$ prediction [17] for quantum $S = 1/2$ autocorrelations at $\beta = 0$ is indicated (thick solid curves). In (b) the numerical $q = \pi/9$ result for the classical *autocorrelation* at $\beta = 0$ is shown for $N = 10000$ (thin solid curve).

increases at fixed A , which is already visible in Figs. 2(a) and (b). However, for $\Delta = 2.0$, the effect is comparatively small for $A = 1/4$ and may completely disappear in the limit of $A \rightarrow 0$. In our CM simulation we cannot consider the case of a very small total amplitude $A \ll 1/4$ since $D_{\pi/9}(t)$ develops strong “oscillations” if A is decreased too much. Such oscillations are already observable for $A = 1/4$ in Fig. 2 and essentially arise from a too small number of initial states, as we will demonstrate later in detail. This observation indicates that averaging is more important for “close-to-equilibrium” states, at least for a chain of finite length. It is worth to mention that M_q is less sensitive to averaging because the integration in Eq. (6) smoothes the oscillatory behavior. For completeness, we illustrate in Fig. 2 (b) the same oscillatory behavior for the classical density-density *correlation* at $\beta = 0$, evaluated according to [26] and sampled over $N = 10000$ completely random initial states (10 times more than before). Despite the still strong oscillations, this correlation is consistent with the decay at $A = 1/4$, which particularly excludes a possibly “far-from-equilibrium” scenario for this choice of A .

So far, the CM results in Figs. 1, 2 can be reproduced for a chain of length $L = 18$ if the averaging is performed over $N \gg 10000$ initial configurations, which is feasible for a short chain. Hence, these results are certainly free of relevant finite-size effects. Next we proceed to smaller momenta $q < \pi/9$, which cannot be realized for $L = 18$

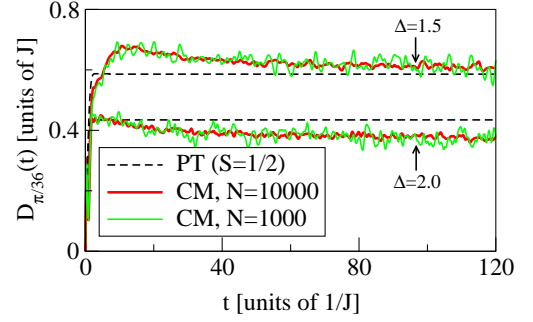


Fig. 3: Time-dependence of the generalized diffusion coefficient $D_{\pi/36}(t)$ for anisotropies $\Delta = 1.5, 2.0$ in a chain of length $L = 18000$, as obtained numerically from classical mechanics for the total amplitude $A = 1/4$ and different averages over $N = 1000$ and 10000 initial states (solid curves). Remaining numerical parameter: $\delta t J = 0.01$. As in Fig. 2, the quantum $S = 1/2$, $\beta = 0$ prediction of the $q \rightarrow 0$ perturbation theory in [17] is indicated (dashed curves).

any further. In Fig. 3 we display the generalized diffusion coefficient $D_q(t)$ at fixed momentum $q = \pi/36$, still for anisotropies $\Delta = 1.5, 2.0$ and the small total amplitude $A = 1/4$. The similarity to the results in Fig. 2 is obvious, even though a wider time window $t J \leq 120$ is plotted in Fig. 3. In this time window, the decrease of $D_{\pi/36}(t)$ appears to stagnate. On that account, without causing a large error, we may consider $D_{\pi/36}(t)$ as an approximately time-independent quantity, which is not identical but at least close to $D_{q \rightarrow 0}$ from the PT in [17]. We have checked in addition that the CM curve for $D_q(t)$ does not change significantly at $q = \pi/18$ or $\pi/72$, although not shown explicitly here. This independence of q , together with the approximative independence of t , is a clear signature of diffusion. This observation is one main result of the work at hand. It indicates the existence of CM diffusion in an extended region of time and momentum in quantitative agreement with QM predictions for $S = 1/2$ at $\beta = 0$. Of course, even smaller q and longer t may be evaluated; however, it is reasonable that the above t - and q -region lies already within the hydrodynamic regime and at some point it is hardly possible to exclude errors due to the applied numerical integrator. In this context we demonstrate finally that “oscillations” of $D_q(t)$ do not refer to such errors but only depend on the number of initial configurations. To this end, Fig. 3 also shows $D_{\pi/36}(t)$ for $N = 10000$, which clearly is smoother than for $N = 1000$.

Next we turn to the isotropic point, i.e., $\Delta = 1$. First, we intend to clarify whether there still is a relationship to $S = 1/2$, $\beta = 0$ density autocorrelations, as done before for $\Delta > 1$ in Fig. 1. However, since the PT in [17] is not applicable in the region $\Delta \sim 1$, we proceed differently and instead obtain these density autocorrelations numerically using ED for a chain of length $L = 18$. To repeat, in such a short chain the smallest realized (non-zero) momentum is $q = \pi/9$. In Fig. 4 the resulting relaxation of density autocorrelations is displayed for momenta $q = 2\pi/9, \pi/9$

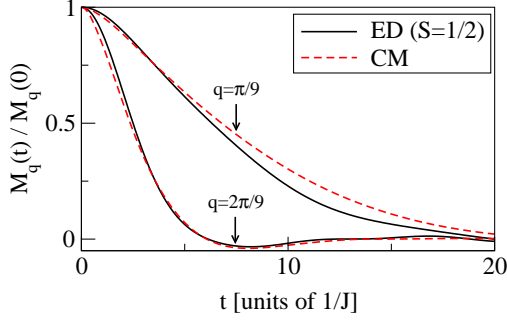


Fig. 4: Relaxation of modes $M_q(t)$ at momenta $q = \pi/9, 2\pi/9$ for the anisotropy $\Delta = 1.0$ in a chain of length $L = 18000$, as obtained numerically from classical mechanics for the total amplitude $A = 1/4$ (non-solid curves). Numerical parameters: $N = 1000$, $\delta t J = 0.01$. For comparison, the decay of quantum $S = 1/2$ autocorrelations at $\beta = 0$ is shown, as found from exact diagonalization for a chain of length $L = 18$.

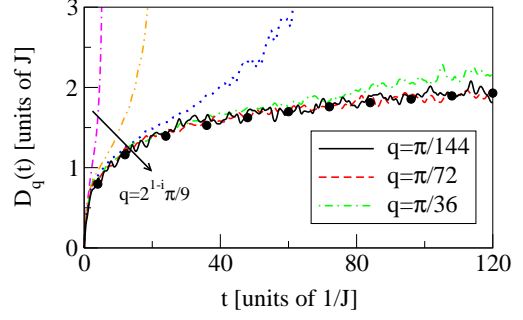


Fig. 5: The generalized diffusion coefficient $D_q(t)$ at momenta $q = 2^{1-i} \pi/9$ ($i = 0, 1, \dots, 5$) for the anisotropy $\Delta = 1$ in a chain of length $L = 18000$, as found numerically from classical mechanics for the total amplitude $A = 1/4$ (using $N = 1000$ initial states and a time step of $\delta t J = 0.01$). For comparison, the function $0.33 [1 + \ln(tJ)]$ is indicated (circles).

and compared with the CM result on the decay of M_q at the same momenta but in a much longer chain of length $L = 18000$. Again, for a small total amplitude $A = 1/4$ the quantitative agreement is remarkably good. Of course, the agreement appears to be much better for the larger momentum $q = 2\pi/9$, where the same slight oscillation around zero is found in CM and QM, emerging at a time scale $tJ \sim 6$. Such oscillations are well known to emerge at large q [22] and zero-crossings yield divergencies of the generalized diffusion coefficient [18], as also visible in later numerical data. For the smaller momentum $q = \pi/9$ the CM and QM curves in Fig. 4 start to deviate from each other at a time scale $tJ \sim 10$; however, finite-size effects of a QM curve for $L = 18$ usually set in at this time scale [18]. On that account the agreement in Fig. 4 supports the relationship between CM and QM, which may also hold in the limit of smaller momenta and longer times.

In Fig. 5 we eventually summarize our CM results on the generalized diffusion coefficient $D_q(t)$ for $\Delta = 1$ over a wide range of momenta $q = 2^{1-i} \pi/9$ ($i = 0, 1, \dots, 5$), i.e., between $2\pi/9$ and $\pi/144$. (Strictly speaking, the smallest momentum reads $q = 2\pi 63/18000 \approx \pi/144$.) Apparently, $D_q(t)$ depends significantly on momentum at $q < \pi/72$ and even diverges because of the slight oscillation of M_q around zero, as already shown in Fig. 4. In the depicted time window, $tJ \leq 120$, a negligible dependence of $D_q(t)$ on momentum is found firstly when varying q from $\pi/72$ to $\pi/144$. Although all CM curves in Fig. 5 are consistent with $D_q(t) \sim D_{\pi/144}(t) + \tilde{q}^4 (tJ)^2/4$, this q -scaling has to be taken as a rule of thumb for the dominant dependence on q without derivation. We emphasize that the CM curve at $q = \pi/144$ agrees well with previous results on CM density-density correlations. For instance, using in Eq. (5) the function $\exp[-0.537 q^2(1 + 0.1 \ln|q|) Jt \ln(Jt)]$, which is one possible fit function in [26] (see also the discussion in [27]), we obtain for $D_{\pi/144}(t)$ a corresponding function $0.33 [1 + \ln(tJ)]$, as indicated in Fig. 5 (circles). Clearly,

the time-dependence of $D_{\pi/144}(t)$ may be a pointer to such a logarithm. Furthermore, because of the good agreement with [26], this logarithmic increase cannot be understood as a “not-close-to-equilibrium” effect resulting from the choice of the total amplitude $A = 1/4$. In fact, we do not find a relevant dependence on A . One might be tempted to speculate on the time- and momentum-dependence of $D_q(t)$ beyond the depicted time window, see also a related discussion in [26,27]; however, it is hardly feasible to verify a possibly logarithmic time-dependence of $D_q(t)$ from a merely numerical simulation. In any case, at least for the considered t and q in Fig. 5 the dynamics turns out to be non-diffusive. In view of the agreement with $S = 1/2$, $\beta = 0$ density autocorrelations in Fig. 4, we may expect a similar dynamics in QM. This expectation has impact on numerical approaches to QM dynamics, simply since most approaches are confined to the here considered t and q , e.g., $q = \pi/144$ represents the smallest momentum in a long chain of length $L = 288$. While this length will never be reached by ED, it may be treatable by time-dependent density matrix renormalization group [21], even though restricted to zero temperature yet. It is worth to mention that a recent result for $L = 256$ from a non-equilibrium bath scenario on the basis of the Lindblad quantum master equation supports superdiffusive transport at $\beta = 0$ [13], which is consistent with Fig. 5.

In summary, we studied the transport of magnetization for the classical Heisenberg chain at and especially above the isotropic point. To this end, we solved the Hamiltonian equations of motion numerically for initial states realizing harmonic-like magnetization profiles of small amplitude and with random phases. Above the isotropic point, i.e., for large anisotropies $\Delta \sim 1.5$ we found that the resulting dynamics of the ensemble average becomes diffusive in a hydrodynamic regime starting at rather small times and large momenta. We further brought the diffusion constant into good quantitative agreement with quantum $S = 1/2$ predictions at high temperatures $\beta = 0$. At the isotropic

point, i.e., for the anisotropy $\Delta = 1$ we did not observe evidence of diffusive dynamics at the considered times and momenta. But even for $\Delta = 1$ we found at large momenta a remarkably good agreement with numerical results for quantum $S = 1/2$ density autocorrelations at $\beta = 0$. On that account we finally argued that our findings for the classical dynamics may also have impact on the quantum dynamics for $\Delta = 1$. While it is questionable if the present classical approach to transport is indeed appropriate to simulate possibly pure and strongly S -dependent quantum effects at low temperatures, the possibility of a classical simulation at not too low temperatures appears to be promising and may be explored further.

* * *

The author sincerely thanks W. Brenig, P. Prelovšek, J. Herbrych, T. Prosen, and M. Žnidarič for interesting and fruitful discussions.

REFERENCES

- [1] CASATI G., FORD J., VIVALDI F. and VISSCHER W. M., *Phys. Rev. Lett.*, **52** (1984) 1861.
- [2] GARRIDO P. L., HURTADO P. I. and NADROWSKI B., *Phys. Rev. Lett.*, **86** (2001) 5486.
- [3] LI B., CASATI G., WANG J. and PROSEN T., *Phys. Rev. Lett.*, **92** (2004) 254301.
- [4] SIRKER J., PEREIRA R. G. and AFFLECK I., *Phys. Rev. Lett.*, **103** (2009) 216602; *Phys. Rev. B*, **83** (2011) 035115.
- [5] ZOTOS X., *Phys. Rev. Lett.*, **82** (1999) 1764.
- [6] HEIDRICH-MEISNER F., HONECKER A., CABRA D. C. and BREINIG W., *Phys. Rev. B*, **68** (2003) 134436.
- [7] BENZ J., FUKUI T., KLÜMPER A. and SCHEEREN C., *J. Phys. Soc. Jpn.*, **74** (2005) 181.
- [8] PROSEN T., *Phys. Rev. Lett.*, **106** (2011) 217206.
- [9] KARRASCH C., BARDARSON J. H. and MOORE J. E., arXiv:1111.4508 (2011).
- [10] FABRICIUS K. and MCCOY B. M., *Phys. Rev. B*, **57** (1998) 8340.
- [11] SIRKER J., *Phys. Rev. B*, **73** (2006) 224424.
- [12] GROSSJOHANN S. and BREINIG W., *Phys. Rev. B*, **81** (2010) 012404.
- [13] ŽNIDARIČ M., *Phys. Rev. Lett.*, **106** (2011) 220601.
- [14] MICHEL M., HESS O., WICHTERICH H. and GEMMER J., *Phys. Rev. B*, **77** (2008) 104303.
- [15] PROSEN T. and ŽNIDARIČ M., *J. Stat. Mech.: Theory Exp.*, **2009** (2009) P02035.
- [16] STEINIGEWEG R. and SCHNALLE R., *Phys. Rev. E*, **82** (2010) 040103R.
- [17] STEINIGEWEG R., *Phys. Rev. E*, **84** (2011) 011136.
- [18] STEINIGEWEG R. and BREINIG W., *Phys. Rev. Lett.*, **107** (2011) 250602.
- [19] PRELOVŠEK P., EL SHAWISH S., ZOTOS X. and LONG M., *Phys. Rev. B*, **70** (2004) 205129.
- [20] MIERZEJEWSKI M., BONČA J. and PRELOVŠEK P., *Phys. Rev. Lett.*, **107** (2011) 126601.
- [21] LANGER S. *et al.*, *Phys. Rev. B*, **79** (2009) 214409.
- [22] FABRICIUS K., LÖW U. and STOLZE J., *Phys. Rev. B*, **55** (1997) 5833.
- [23] MÜLLER G., *Phys. Rev. Lett.*, **60** (1988) 2785.
- [24] GERLING R. W. and LANDAU D. P., *Phys. Rev. Lett.*, **63** (1989) 812.
- [25] GERLING R. W. and LANDAU D. P., *Phys. Rev. B*, **42** (1990) 8214.
- [26] DE ALCANTARA BONFIM O. F. and REITER G., *Phys. Rev. Lett.*, **69** (1992) 367; *Phys. Rev. Lett.*, **70** (1993) 249.
- [27] BÖHM M., GERLING R. W. and LESCHKE H., *Phys. Rev. Lett.*, **70** (1993) 248.
- [28] BETHE H., *Z. Phys. A*, **71** (1931) 205.
- [29] SOLOGUBENKO A. V. *et al.*, *Phys. Rev. Lett.*, **84** (2000) 2714.
- [30] HESS C. *et al.*, *Phys. Rev. B*, **64** (2001) 184305.
- [31] HLUBEK N. *et al.*, *Phys. Rev. B*, **81** (2010) 20405R.
- [32] THURBER K. R., HUNT A. W., IMAI T. and CHOU F. C., *Phys. Rev. Lett.*, **87** (2001) 247202.
- [33] KÜHNE H. *et al.*, *Phys. Rev. B*, **80** (2009) 045110.
- [34] ARNOLD V. I., *Mathematical Methods of Classical Mechanics* (Springer) 1978.
- [35] STEINIGEWEG R. and SCHMIDT H.-J., *Math. Phys. Anal. Geom.*, **12** (2009) 19.
- [36] MAHAN G. D., *Many Particle Physics* (Springer) 2000.